

Negative permittivity derived from inductive characteristic in percolating copper/epoxy resin metacomposites

Kai Sun ¹, Jiahao Xin ¹, Yaping Li ¹, Zhongyang Wang ^{2,3}, Qing Hou ^{4*}, Xiaofeng Li ¹, Xinfeng Wu ¹, Runhua Fan ^{1,2*}, Kwang Leong Choy ^{5*}

¹*College of Ocean Science and Engineering, Shanghai Maritime University, Shanghai 201306, China*

²*Key Laboratory for Liquid-Solid Structural Evolution and Processing of Materials (Ministry of Education), Shandong University, Jinan 250061, China*

³*Department of Materials Science and Engineering, National University of Singapore, Singapore 119077, Singapore*

⁴*Department of Chemistry, University College London, London WC1H 0AJ, UK.*

⁵*UCL Institute for Materials Discovery, University College London, London WC1E 7JE, UK.*

* Corresponding author.

E-mail address: qing.hou.16@ucl.ac.uk (Q. Hou); fan@sdu.edu.cn (R.H. Fan); k.choy@ucl.ac.uk (K.L. Choy)

Recently, increasing attention has been concentrated on negative permittivity with the development of the emerging metamaterials composed of periodic array structures. However, taking facile preparation into consideration, it is important to achieve negative permittivity behavior based on materials' intrinsic properties rather than their artificially periodic structures. In this paper, we proposed to fabricate the percolating copper/epoxy resin (Cu/EP) composites by a polymerization method to realize the negative permittivity behavior. When Cu content in the composites reached to 80 wt.%, the conductivity abruptly went up by three orders of magnitudes, suggesting a percolation behavior. Below the percolation threshold, the conductivity spectra conform to Jonscher's power law; when the Cu/EP composites reached to percolating state, the conductivity gradually reduced in

high frequency region due to the skin effect. It is indicated that the conductive mechanism changed from hopping conduction to electron conduction. In addition, the permittivity did not increase monotonously with the increase of Cu content in the vicinity of percolation threshold, due to the presence of leakage current. Meanwhile, the negative permittivity conforming to Drude model was observed above the percolation threshold. Further investigation revealed that there was a constitutive relationship between the permittivity and the reactance. When conductive fillers are slightly above the percolation threshold, the inductive characteristic derived from conductive percolating network leads to the negative permittivity. Such epsilon-negative materials can potentially be applied in novel electrical devices, such as high-power microwave filters, stacked capacitors, negative capacitance field effect transistors and coil-free resonators. In addition, the design strategy based on percolating composites provides an approach to epsilon-negative materials.

Key words: Negative permittivity; Epsilon-negative materials; Percolating composites; Metacomposites; Metamaterials

1. Introduction

Permittivity is one constitutively physical parameter that describes the interaction of a material with an electric field. Generally, it requires different dielectric properties to meet diverse application requirements ^[1]. For example, capacitors require the high permittivity and low dissipation ^[2], while a large dissipation with moderate permittivity is suitable for microwave absorption ^[3]. Moreover, the dielectric constant and dissipation in wave-transmitting materials are commonly small ^[4]. In the past, nearly all of the investigations focused on the positive permittivity, while less attention was paid to the negative permittivity until Veselago hypothesized the theoretical possibility of negative refraction ^[5]. It has been indicated that the epsilon-negative materials have

great potential applications for high-power microwave filters ^[6], novel capacitors with high permittivity ^[7], negative capacitance field effect transistors ^[8] and coil-free resonators ^[9], *etc.*

It is indicated that negative permittivity can be generated by plasma, which is an established collective excitation of metals in the visible or near ultraviolet region ^[10]. However, for pure metals, the negative permittivity is too huge at a lower frequency region; meanwhile, the dissipation is several orders of magnitude greater than the permittivity, leading to the fact that the complex permittivity is essentially imaginary ^[11]. Pendry ^[12] has theoretically proposed to embed very thin metal wires into periodic structures to dilute the electron density and considerably enhance the effective electron mass through self-inductance, finally reducing the plasma frequency to microwave frequency region. According to this idea, Smith *et al.* ^[13] have experimentally built periodic structures with split ring resonators and metal wires, which also called metamaterials, to attain negative permittivity in microwave frequency region. Since then, more attention has been focused on negative permittivity with the development of the emerging metamaterials ^[14, 15], which are artificially fabricated via periodic structure units on a subwavelength scale and gain unique properties from their periodic structures rather than from their intrinsic compositions and microstructures ^[16].

As an extension for periodic metamaterials, it has become a prevalent research focus to achieve negative permittivity behavior in random materials by taking advantage of their intrinsic properties ^[17-19]. These random materials with negative electromagnetic parameters are termed as intrinsic metamaterials or metacomposites ^[20], which can be fabricated via typical materials techniques, and their properties are effectively controlled by tailoring chemical compositions and microstructures ^[21-22]. Meanwhile, metacomposites exhibit an isotropic electromagnetic response due to their homogeneity. Fan *et al.* ^[23-26] fabricated ceramic-based composites with different conductive metals (*e.g.*, Ni, Fe, Ag) and carbon materials (*e.g.*, carbon nanotubes, graphene and amorphous carbon) to realize negative permittivity. Tsutaoka *et al.* ^[27] have prepared permalloy/polyphenylene sulfide composites and attained negative permittivity in microwave frequency region. Guo *et al.* ^[28, 29] have employed in-situ polymerization process to achieve conductive polymer matrix epsilon-negative materials. Qiu *et al.* ^[30] have selected carbon nanotubes as functional fillers to attain negative permittivity in polymer composites. It is indicated that the negative permittivity can be observed due to the plasma oscillation of the conduction electrons from conductive materials ^[31]. The electron

transport property can be presented in the form of a specific microcircuit, so it is important to clarify the generation mechanism of negative permittivity from the perspective of a microcircuit.

Moreover, compared with those of ceramic materials, polymers have added advantages in processing and application in the field of electronic devices. Herein we proposed to exploit percolating composites to fabricate polymer-based epsilon-negative materials. It is well known that there are huge contrasts especially in electrical properties between metals and polymers. When metal particles are embedded into an insulating polymer matrix, the conductive particles can form a continuous network throughout the system. Along with the percolation phenomenon of the microstructure, it is feasible to observe the negative permittivity in percolating composites by tuning their compositions and tailoring their microstructures. Among metallic functional fillers, copper could be an appropriate candidate to offer conduction electrons for negative permittivity owing to its excellent conductivity and chemical stability^[32]. Meanwhile, epoxy resin has great value of electrical/electronic devices due to their tremendous electrical resistivity, excellent mechanical property and low manufacturing cost^[33], which could be an appropriate candidate to dilute the electron density of pure Cu.

In this paper, the percolating Cu/EP composites were fabricated to obtain negative permittivity via a facile polymerization process. The negative permittivity was observed when Cu content reached to percolation threshold. The conduction mechanism of the resulting composites changed from hopping conduction to electron conduction. Further investigation revealed a corresponding relationship between the permittivity and the impedance. Specifically, the negative permittivity was attributed to the inductive characteristic derived from the conductive percolating network.

2. Experimental

2.1 Preparation Process.

In this work, epoxy resin E51 (bisphenol A epoxy) and curing agent T31 were purchased from Shandong Yousuo Chemical Co., Ltd (China). The micro-sized Cu sheets with an average size of about 45 μm were chosen as the functional fillers, which were purchased from Shanghai Puwei Applied Materials Technology Co., Ltd (China). All materials were used as

received without any further treatment.

The epoxy resin, curing agent and absolute ethyl alcohol (regarded as the solvent) were mixed in the beaker with a mass ratio of 10:1:4. Then the mixture added with different mass fractions of flaky Cu particles (0, 10, 30, 50, 70, 75 and 80 wt.%), which were denoted as samples 0%, 10%, 30%, 50%, 70%, 75% and 80%, respectively. The mixture was treated in water bath at 60 °C, and stirred at a speed of 600 rpm for 2 h. Subsequently, the mixture was poured into the silicone rubber mold with a dimension of 20 mm in diameter. The suspension was vacuumized and kept in vacuum dry oven for 30 min to eliminate the bubbles. The curing process of composites involved three steps to improve their curing performance: kept them at 60 °C for 1 h; then at 90 °C for 2 h, and finally at 120 °C for 5 h. After cooling them down naturally to room temperature, the Cu/EP composites were produced.

2.2 Characterization and Measurement.

The microstructures of the resulting composites were observed by scanning electron microscopy (SEM, FEI Quanta 650). The phase identification of the composites was performed by X-ray diffraction (XRD; Tokyo, Japan) using the Rigaku D/max-rB X-ray with Cu K α radiation. Thermogravimetric analysis (TGA) of the resulting composites was investigated using a synchronous thermal analyzer (Netzsch, STA 499 F3 Jupiter) in the range of temperature from room temperature to 500 °C, which was carried out at a heating rate 10 °C/min in nitrogen atmosphere.

Dielectric properties of the Cu/EP composites were measured by a parallel plate method, also called the three-terminal method, at room temperature using Keysight E4980AL LCR meter (Keysight Technologies Co. Ltd., USA) in the frequency from 10 kHz to 1 MHz. In order to eliminate the stray capacitance derived from the edge of the sample, the main electrode was protected by a guard electrode, which could absorb the electric field at the edge. Platinum film was sputtered on both sides of the samples to reduce the measurement error derived from airgap. The upper film electrode was processed into annulus, in which the inner diameter was 10 mm and the gap between the inner and outer circles was about 1 mm. Before testing, the platinum coating on the surrounding of the samples was removed by polishing to avoid short circuit. Subsequently, the open and short compensation were carried out to eliminate the stray admittance and residual impedances of the test fixtures, respectively. Afterwards, the electrodes were adjusted to be parallel. After compensation and adjustment, the samples were in contact with the two electrodes for measurement. The measured data

including capacitance C and resistance R were used to calculate permittivity ε_r' and AC conductivity σ_{ac} , which can be expressed as follows,

$$\sigma_{ac} = \frac{t}{RS} \quad (1)$$

$$\varepsilon_r' = \frac{tC}{A\varepsilon_0} \quad (2)$$

where R , C , S , A , t and ε_0 are resistance, capacitance, the area of samples, the area of the electrode, the thickness of samples and the vacuum permittivity (8.85×10^{-12} F/m), respectively. The electrical conductivity spectra were in the frequency range of 20 Hz - 1 MHz.

3. Results and discussion

The phase composition and microstructure of the Cu/EP composites are shown in **Fig. 1**. As shown in **Fig. 1a**, for pure epoxy resin, there is a broad diffraction peak in the low angle range ($10^\circ < 2\theta < 20^\circ$), which indicated an amorphous structure. With the increase of Cu content, the broad peak of epoxy resin was gradually masked by the strong intensity of the diffraction peak of Cu. The characteristic peaks of Cu (JCPDS card #04-0836) were observed in the resulting composites, and there were no shifts in the Cu peaks, which suggested that no unexpected reaction took place during the preparation process. Therefore, the Cu/EP composites were fabricated via in-situ synthesis procedure. The microstructures of the Cu/EP composites were presented in **Fig. 1b-e**. When Cu content was located at a low loading level, the isolated Cu sheets were randomly embedded in the polymer matrix (**Fig. 1b**). With the increase of Cu sheets, the conductive fillers interconnected together and formed an aggregation (**Fig. 1c**). Further increasing the fraction of Cu, the microsized Cu sheets came into contact and established continuous networks in the Cu/EP composites (**Fig. 1d-f**). It was demonstrated that there was an obvious change of microstructure, *i.e.*, percolation phenomenon. In general, the electrical properties of polymer-conductor composites undergo an abrupt shift along with the change of microstructure. Hence, the dependence of conductivity and permittivity in the Cu/EP composites on their composition and microstructure are further studied in the following section.

The TGA of the Cu/EP composites was investigated since the thermal stability of materials can have a significantly impact on the reliable performances of devices. TGA curves of the Cu/EP

composites are shown in **Fig. 2**. It can be seen that the resulting composites began to decompose at about 350 °C, and was nearly close to complete decomposition at about 460 °C. Below 350 °C, water evaporation and some oligomer decomposition led to a slightly decreased weight of pure epoxy resin. In the range of 350 °C and 460 °C, the molecular chains of epoxy resin were significantly destroyed and gave rise to a rapid decomposition of epoxy resin. Hence there was an abrupt decrease of weight during the heating process. When the temperature was up to 460 °C, the TGA curves were gradually prone to be stable, which indicated that the thermal decomposition was nearly terminated. In addition, the ultimate residual weights of the Cu/EP composites were obviously larger than that of pure epoxy resin. As shown in **Fig. 2b**, with the increase of Cu content, the residual weight was not expected to monotonically increase. When a small amount of flaky Cu particles were incorporated into epoxy resin, the thermal decomposition rate was lessened, which resulted from the crosslink action between epoxy resin and copper. Meanwhile, during the heating process, Cu played a primary role in improving the heat resistance due to its higher decomposition temperature and heat capacity. When the fillers were at a high level, it was detrimental to the enhancement of crosslink between epoxy resin and copper. Therefore, the thermal stability of the resulting composites with higher Cu content gradually decreased. As compared with that of pure epoxy resin, the thermal stability of the Cu/EP composites was eventually enhanced at a temperature below 300 °C. It is demonstrated that the Cu/EP composites can ensure a reliable performance in a wide scope of temperature.

Fig. 3 shows the electrical conductivity of the Cu/EP composites with different Cu content. Compared with that of pure epoxy resin, the electric conductivities of the resulting composites measured at the beginning of the test frequency increased when Cu sheets were introduced into the polymer matrix. It is worth noting that the conductivity monotonically increased with the increase of the frequency, when Cu content is at a relatively low ratio. Further analysis on this phenomenon indicated that conductivity spectra conformed to Jonscher's power law ^[34], which can be described as the following equation, $\sigma_{ac}(\omega) = \sigma_{dc} + A\omega^n$. As shown in **Fig. 3a**, the fitted data are in good accordance with the measured results based on this equation. The electrons in the Cu/EP composites moved along the conductive particles in the form of a discontinuous hopping. In a higher frequency region, the electrons can obtain more energy, which contributes to their hopping conduction, resulting in the enhancement of electric conductivity ^[35]. In addition, the conductivity of the resulting composites measured at 20 Hz is shown in **Fig. 3b**. It is demonstrated that Cu sheets formed a

conductive network and the conductivity abruptly went up by three orders of magnitude when Cu content in the composites reached to 80 *wt.%*, which implies that there is an electrical percolation behavior in the Cu/EP composites. Compared with previous investigation ^[36], the smaller size of conductive fillers contributed to the formation of percolating network. Moreover, the electric conductivity gradually reduced with the increase of frequency, which was attributed to the skin effect. Specifically, the resistance can become enlarged due to the decrease of skin depth in the higher frequency region ^[37]. Hence, the conductivity gradually got lessened with the increase of frequency. Along with the microstructural transformation of the resulting composites, the conductive mechanism of the resulting composites changed from hopping conduction to electron conduction. The similar phenomenon was also observed in percolating ceramic-based composites ^[4, 38].

The permittivity spectra of the Cu/EP composites are shown in **Fig. 4**. In contrast to pure epoxy resin, the dielectric constant of the resulting composites got enlarged with the increase of Cu content. When conductive fillers were added into the insulating epoxy resin, the charges gathered round the interfaces between Cu and polymer. The interfaces between conductive fillers and matrix can be equivalent to numerous microcapacitors, which were responsible for the increase of permittivity. The permittivity of the Cu/EP composites was enhanced owing to the interfacial polarization, which is also called Maxwell-Wagner-Sillars effect ^[39]. The similar phenomenon is also observed in silver/alumina composites ^[40]. Interestingly, the permittivity spectra for the composites with a low content of flaky Cu particles exhibited “flat” dielectric response with a frequency-independence behavior. The frequency response from the polymer matrix was still overwhelming when the content of Cu fillers was at a low loading level. In general, the dielectric constant maintained at a stable value in a wide scope of frequency, which is beneficial to the reliability of dielectric property. However, when the fraction of Cu fillers was in the vicinity of the percolation threshold, the permittivity spectrum of the Cu/EP composites with 70 *wt.%* Cu presented obvious dielectric dispersion. The similar phenomenon was also observed in the composites with carbon nanoparticles ^[41] or multi-walled carbon nanotubes ^[42]. As is well known, dielectric constant is determined by the polarization of dipoles. The excessive conductive particles suppressed the motion of dipoles, so it was difficult for dipoles to follow the change of external field, which brought about the decrease of permittivity in the high frequency region.

When the mass fraction of Cu sheets reached up to 75 wt.%, the permittivity was smaller than that of the resulting composites with 70 wt.% Cu (**Fig. 4a**). It seems a little abnormal, but it still makes sense. With regard to this point, it can be attributed to the presence of leakage current among the composites. As mentioned above, permittivity, which describes the interaction of a material with an electric field, is dependent on the polarization of dipoles. When the conductive fillers are in the vicinity of the percolation threshold, the interconnected Cu sheets can form an aggregation and generate leakage current, which is unexpected for the polarization of dipoles. Therefore, the permittivity did not increase further for the sample with 75 wt.% Cu. In other word, the permittivity did not increase monotonously due to the presence of leakage current especially in the vicinity of the percolation threshold, when incorporating more Cu into the insulating epoxy resin. When further increasing Cu content, negative permittivity was observed in the overall test frequency range (**Fig. 4b**). The similar phenomenon was also observed in copper/yttrium iron garnet composites [32]. It is indicated that the inversion of permittivity from positive to negative belongs to a continuous change rather than a discontinuous change.

Combined with the SEM image of the Cu/EP composites (**Fig. 1f**), it is indicated that there is a close relationship between the continuous conductive network and the negative permittivity. The conduction electrons played an important role in negative permittivity. In theory, the plasma-like negative permittivity behavior can be investigated by Drude model as follows [24],

$$\varepsilon_r'(\omega) = 1 - \frac{\omega_p^2}{\omega^2 + \omega_\tau^2} \quad (3)$$

$$\omega_p = \sqrt{\frac{ne^2}{m\varepsilon_0}} \quad (4)$$

where ω_p is the plasma angular frequency, ω_τ is the collision frequency (the inverse relaxation time $1/\tau$), ω is the test angular frequency, n is the effective electron density, m is the effective mass, ε_0 is the vacuum permittivity and e is the electron charge (1.6×10^{-19} C).

The electrons in conductors would give rise to a collective oscillation due to the combined effects of their own inertia and restoring force. The characteristic frequency, in which the electrons produce

the plasma oscillation, is termed as plasma frequency. In general, negative permittivity is commonly observed below the plasma frequency. For bulk metals, their plasma frequency is usually in the visible or ultraviolet region^[10]. Hence, the absolute values of negative permittivity for bulk Cu are very huge ($\sim 10^6$) in radio frequency region, which is ascribed to their ultrahigh electron density^[32]. In this work, the micro-sized Cu sheets were embedded in insulating epoxy resin, leading to the dilution of electron density. As compared with that of the copper/polyphenylene sulfide composites^[18], the negative permittivity of the Cu/EP composites was dramatically decreased in radio frequency range. The Drude-like negative permittivity was also achieved in polypyrrole/tungsten oxide composites^[43]. It is well known that the electron transport property can be presented with a specific microcircuit. Therefore, in order to further reveal the generation mechanism of negative permittivity behavior from the perspective of microelectronics, the relationship between impedance and permittivity was further investigated.

Fig. 5 shows the complex impedance spectra of the Cu/EP composites. The real and imaginary part of impedance means resistance and reactance, respectively. When reactance is negative value, the resulting composites show capacitive characteristic, indicating that the voltage phase lags behind the current phase. While for the reactance with positive value, it possesses inductive characteristic^[44]. In the resulting composites with positive permittivity, the reactance was negative value at the corresponding frequency region (**Fig. 5a**). As shown in **Fig. 5b**, the reactance is positive value, which is corresponded to negative permittivity in **Fig. 4b**. Therefore, there is a close relationship between the permittivity and the reactance. In previous investigation^[45], the impedance property of materials is associated with their microelectronics, thus the circuit models of the Cu/EP composites were further investigated based on equivalent circuit analysis. It can be seen that the fitted data (the red solid lines) are in good agreement with the measured results. Interestingly, with the increase of Cu content, the impedance module significantly decreased, which suggests that the conductivity has been gradually enhanced. As shown in the inset of **Fig. 5a**, below the percolation threshold, the resulting composites can be equivalent to the circuits, which were composed of a series resistor R_1 , a parallel resistor R_2 and a capacitor C . The resistors derived from the contact resistance and the interface resistance, corresponding to R_1 and R_2 , respectively^[46]. The capacitor results from the interface between discontinuous copper and epoxy resin. When the discontinuous Cu sheets embedded in the insulating epoxy resin, it can generate a great deal of microcapacitors. In **Fig. 5b**, the equivalent circuit of the

resulting composites with high content Cu was composed of parallel resistors, capacitor and inductor. Compared with that of the composites with low content Cu, the inductor appeared in the composites with the negative permittivity behavior. It is reported that the inductor is an attribute of a closed loop [47], which is produced by the conductive networks in the Cu/EP composites. Hence, the conduction electrons in the conductive Cu network are responsible for the inductor, while the capacitor depends on polarized electrons [48].

It was implied that there was a constitutive relationship between the permittivity and the reactance, which could be expressed as follows [49],

$$\varepsilon'_r = -\frac{Z''}{2f\pi C_0(Z'^2+Z''^2)} \quad (5)$$

where ε'_r is the real permittivity, Z' , Z'' is the real and imaginary impedance, f is the test frequency and C_0 is the capacitance of vacuum, respectively. The permittivity is dependent on the reactance. Specifically, when the reactance Z'' is negative value, the positive permittivity behavior appears; when the reactance Z'' is positive value, it brings about the negative permittivity. In summary, the capacitive characteristic leads to the positive permittivity, and the inductive characteristic is responsible for the negative permittivity. Similarly, the corresponding relationship between the permittivity and the reactance was also observed in carbon nanotubes/alumina composites[25]. It is well known that the inductive reactance can be enhanced, and the capacitive reactance is restrained under the action of high-frequency electric field. Hence, with the increase of frequency, the absolute values of reactance significantly decrease in the resulting composites with positive permittivity (**Fig. 5a**), while the reactance would increase in the composites with negative permittivity (**Fig. 5b**).

4. Conclusions

In this paper, epoxy resin-based composites with different microsized Cu sheets content were fabricated via a polymerization process. The electrical conduction went up an abrupt enhancement along with the formation of percolating network, when the Cu content in the composites reached to 80 wt.%. Below the percolation threshold, the AC conductivity spectra conform to Jonscher's power law. While above the percolation threshold, the conductivity gradually got lessened in high frequency due to the skin effect, which means that the conductive mechanism of the resulting composites

changes from hopping conduction to electron conduction with the increase of Cu content. In the vicinity of the percolation threshold, the permittivity did not increase monotonously with the increase of Cu content, due to the presence of leakage current. Beyond the percolation threshold, the Drude-like negative permittivity was observed in the percolating composites, which is attributed to the plasma oscillation of electrons in the resulting composites. It revealed that there was a constitutive relationship between the permittivity and the reactance. The positive permittivity results from the capacitive characteristic, while the negative permittivity is ascribed to the inductive characteristic. When conductive fillers are slightly above the percolation threshold, the inductive characteristic derived from conductive percolating network leads to the negative permittivity. The design strategy based on percolating composites provides an approach to epsilon-negative materials, which can be controllable by adjusting their compositions and tailoring their microstructures. The percolating composites with negative permittivity can be a promising candidate for novel electrical devices in the field of capacitors, high-power microwave filters, negative capacitance field effect transistors and coil-free resonators.

Acknowledgements

This work was sponsored by the National Natural Science Foundation of China (Grant No. 51803119, 51871146 and 51771108), the Innovation Program of Shanghai Municipal Education Commission (Grant No. 2019-01-07-00-10-E00053), “Chenguang Program” supported by Shanghai Education Development Foundation and Shanghai Municipal Education Commission (Grant No. 18CG56), and the Science and Technology Commission of Shanghai Municipality (Grant No. 18DZ1112902, No. 18DZ1100802). Thank you also for the helpful comments and suggestions by the reviewers on the paper.

References

- [1] Z.M. Dang, J.K. Yuan, J.W. Zha, T. Zhou, S.T. Li, G.H. Hu, *Prog. Mater. Sci.* 57 (2012) 660-723.
- [2] Z.M. Dang, J.K. Yuan, S.H. Yao, R.J. Liao, *Adv. Mater.* 25 (2013) 6334-6365.
- [3] L. Liu, X. Chen, J. Wang, L. Qiao, S. Gao, K. Song, C. Zhao, X. Liu, D. Zhao, F. Pan, *J. Mater. Sci. Technol.* 35 (2019) 1074-1080.
- [4] X. Wang, Z. Shi, M. Chen, R. Fan, K. Yan, K. Sun, S. Pan, M. Yu, *J. Am. Ceram. Soc.* 97 (2014)

3223-3229.

- [5] V.G. Veselago, *Sov. Phys. Usp.* 10 (1968) 509-514.
- [6] C.H. Liu, N. Behdad, *J. Appl. Phys.* 113 (2013) 064909.
- [7] Z. Shi, J. Wang, F. Mao, C. Yang, C. Zhang, R. Fan, *J. Mater. Chem. A* 5 (2017) 14575-14582.
- [8] A. I. Khan, D. Bhowmik, P. Yu, S. Joo Kim, X. Pan, R. Ramesh, S. Salahuddin, *Appl. Phys. Lett.* 99 (2011) 113501.
- [9] A.I. Khan, K. Chatterjee, B. Wang, S. Drapcho, L. You, C. Serrao, S.R. Bakaul, R. Ramesh, S. Salahuddin, *Nat. Mater.* 14 (2015) 182.
- [10] M. Gao, Z. Shi, R. Fan, L. Qian, Z. Zhang, J. Guo, *J. Am. Ceram. Soc.* 95 (2012) 67-70.
- [11] J.B. Pendry, *Phys. Rev. Lett.* 85 (2000) 3966.
- [12] J.B. Pendry, A. Holden, W. Stewart, I. Youngs, *Phys. Rev. Lett.* 76 (1996) 4773.
- [13] R.A. Shelby, D.R. Smith, S. Schultz, *Science* 292 (2001) 77-79.
- [14] D. Schurig, J. Mock, B. Justice, S.A. Cummer, J.B. Pendry, A. Starr, D.R. Smith, *Science* 314 (2006) 977-980.
- [15] S. Sun, Q. He, S. Xiao, Q. Xu, X. Li, L. Zhou, *Nat. Mater.* 11 (2012) 426.
- [16] K. Sun, R. Fan, X. Zhang, Z. Zhang, Z. Shi, N. Wang, P. Xie, Z. Wang, G. Fan, H. Liu, et al., *J. Mater. Chem. C* 6 (2018) 2925-2943.
- [17] P. Xie, Z. Zhang, K. Liu, L. Qian, F. Dang, Y. Liu, R. Fan, X. Wang, S. Dou, *Carbon* 125 (2017) 1-8.
- [18] T. Tsutaoka, T. Kasagi, S. Yamamoto, K. Hatakeyama, *Appl. Phys. Lett.* 102 (2013) 181904.
- [19] X. Zhang, X. Yan, Q. He, H. Wei, J. Long, J. Guo, H. Gu, J. Yu, J. Liu, D. Ding, *ACS Appl. Mater. Inter.* 7 (2015) 6125-6138.
- [20] K. Sun, P. Xie, Z. Wang, T. Su, Q. Shao, J. Ryu, X. Zhang, J. Guo, A. Shankar, J. Li, et al., *Polymer* 125 (2017) 50-57.
- [21] P. Xie, Z. Zhang, Z. Wang, K. Sun, R. Fan, *Research* 2019 (2019) 1021368.
- [22] H. Gu, X. Xu, M. Dong, P. Xie, Q. Shao, R. Fan, C. Liu, S. Wu, R. Wei, *Carbon* 147 (2019), 550-558.
- [23] Z. Shi, R. Fan, Z. Zhang, L. Qian, M. Gao, M. Zhang, L. Zheng, X. Zhang, L. Yin, *Adv. Mater.* 24 (2012) 2349-2352.
- [24] Z. Shi, R. Fan, K. Yan, K. Sun, M. Zhang, C. Wang, X. Liu, X. Zhang, *Adv. Funct. Mater.* 23

(2013) 4123-4132.

- [25] C. Cheng, R. Fan, Y. Ren, T. Ding, L. Qian, J. Guo, X. Li, L. An, Y. Lei, Y. Yin, et al., *Nanoscale* 9 (2017) 5779-5787.
- [26] K. Sun, R. Fan, Z. Zhang, K. Yan, X. Zhang, P. Xie, M. Yu, S. Pan, *Appl. Phys. Lett.* 106 (2015) 172902.
- [27] T. Tsutaoka, H. Massango, T. Kasagi, S. Yamamoto, K. Hatakeyama, *Appl. Phys. Lett.* 108 (2016) 191904.
- [28] H. Gu, Y. Huang, X. Zhang, Q. Wang, J. Zhu, L. Shao, N. Haldolaarachchige, D. Young, S. Wei, Z. Guo, *Polymer* 53 (2012) 801-809.
- [29] H. Gu, J. Guo, Q. He, Y. Jiang, Y. Huang, N. Haldolaarachchige, Z. Luo, D.P. Young, S. Wei, Z. Guo, *Nanoscale* 6 (2014) 181-189.
- [30] X. Yao, X. Kou, J. Qiu, *Carbon* 107 (2016) 261-267.
- [31] K. Sun, Z.D. Zhang, R.H. Fan, M. Chen, C.B. Cheng, Q. Hou, X.H. Zhang, Y. Liu, *RSC Adv.* 5 (2015) 61155-61160.
- [32] K. Sun, Z. Zhang, L. Qian, F. Dang, X. Zhang, R. Fan, *Appl. Phys. Lett.* 108 (2016) 061903.
- [33] A. Allaoui, S. Bai, H.M. Cheng, J. Bai, *Compos. Sci. Technol.* 62 (2002) 1993-1998.
- [34] A.K. Jonscher, *Nature.* 267 (1977) 673.
- [35] J. Dong, Z. Wang, K. Sun, Q. Jiang, P. Xie, G. Fan, Y. Qu, L. An, R. Fan, *J. Mater. Sci-Mater. El.* 29 (2018) 20832-20839.
- [36] Q. Hou, K. Sun, P. Xie, K. Yan, R. Fan, Y. Liu, *Mater. Lett.* 169 (2016) 86-89.
- [37] Y. Qu, G. Fan, D. Liu, Y. Gao, C. Xu, J. Zhong, P. Xie, Y. Liu, Y. Wu, R. Fan, *J. Alloy. Compd.* 743 (2018) 618-625.
- [38] R. Yin, H. Wu, K. Sun, X. Li, C. Yan, W. Zhao, Z. Guo, L. Qian, *J. Phys. Chem. C* 122 (2018) 1791-1799.
- [39] N. Yousefi, X. Sun, X. Lin, X. Shen, J. Jia, B. Zhang, B. Tang, M. Chan, J.K. Kim, *Adv. Mater.* 26 (2014) 5480-5487.
- [40] Z. Shi, F. Mao, J. Wang, R. Fan, X. Wang, *Rsc Adv.* 5 (2015) 107307-107312.
- [41] H. Huang, Y. Gao, C. Fang, A. Wu, X. Dong, B. Kim, J. Byun, G. Zhang, D. Zhou, *J. Mater. Sci. Technol.* 34 (2018) 496-502.
- [42] Y. Hu, R. Jiang, J. Zhang, C. Zhang, G. Cui, *J. Mater. Sci. Technol.* 34 (2018) 886-890.

- [43] J. Zhu, S. Wei, L. Zhang, Y. Mao, J. Ryu, P. Mavinakuli, A.B. Karki, D.P. Young, Z. Guo, J. Phys. Chem. C 114 (2010) 16335-16342.
- [44] K. Yan, R. Fan, Z. Shi, M. Chen, L. Qian, Y.l. Wei, K. Sun, J. Li, J. Mater. Chem. C 2 (2014) 1028-1033.
- [45] Z. Shi, R. Fan, Z. Zhang, K. Yan, X. Zhang, K. Sun, X. Liu, C. Wang, J. Mater. Chem. C 1 (2013) 1633-1637.
- [46] P. Xie, K. Sun, Z. Wang, Y. Liu, R. Fan, Z. Zhang, G. Schumacher, J. Alloy. Compd. 725 (2017) 1259-1263.
- [47] H. Wu, Y. Qi, Z. Wang, W. Zhao, X. Li, L. Qian, Compos. Sci. Technol. 151 (2017) 79-84.
- [48] K. Sun, R. Fan, Y. Yin, J. Guo, X. Li, Y. Lei, L. An, C. Cheng, Z. Guo, J. Phys. Chem. C 121 (2017) 7564-7571.
- [49] S. Sharma, T. Basu, A. Shahee, K. Singh, N. Lalla, E. Sampathkumaran, J. Alloy. Compd. 663 (2016) 289-294.

Figure and table captions

Fig. 1. Phase identification and the microstructures of the Cu/EP composites. (a) the XRD patterns, (b–f) the SEM images of the Cu/EP composites with 10, 30, 50, 70, and 80 *wt* % Cu content, respectively.

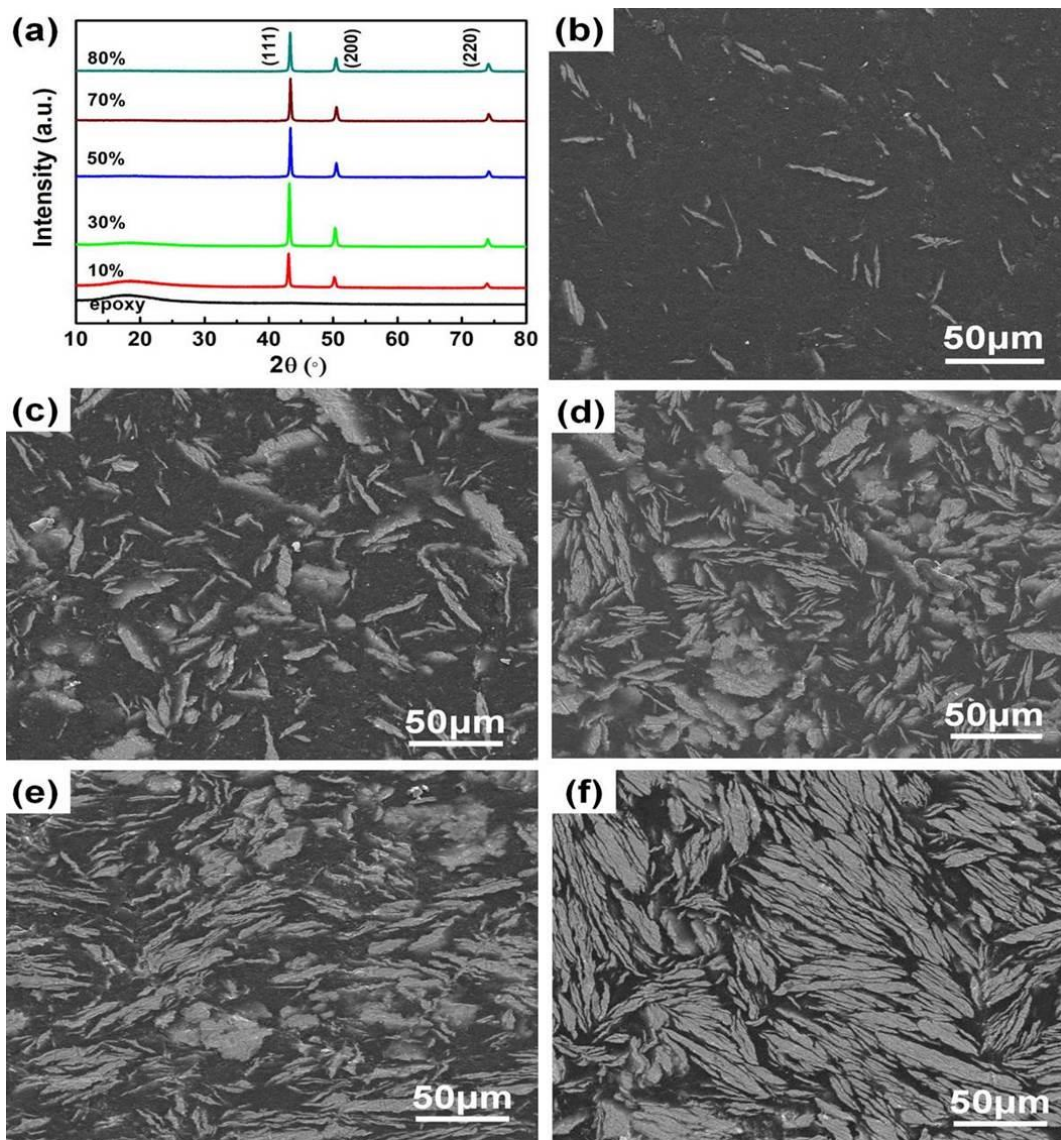


Fig. 2. The TGA curves (a) and partial enlarged views (b) of the Cu/EP composites with different Cu content (*i.e.*, 0-80 *wt.*%).

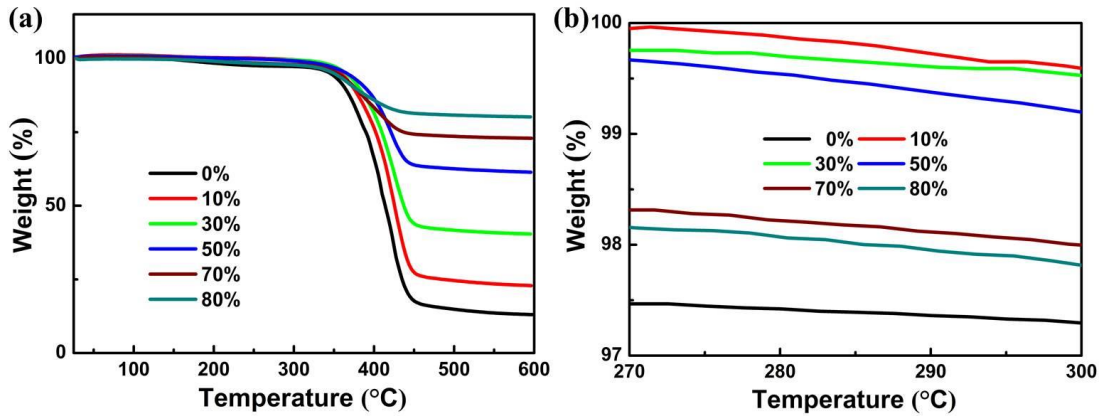


Fig. 3. The electrical conductivities of the Cu/EP composites with different Cu content (*i.e.*, 0-80 wt.%). (a) AC conductivity spectra, and the solid lines show the fitted results. (b) the dependence of conductivity on copper content (measured at 20 Hz).

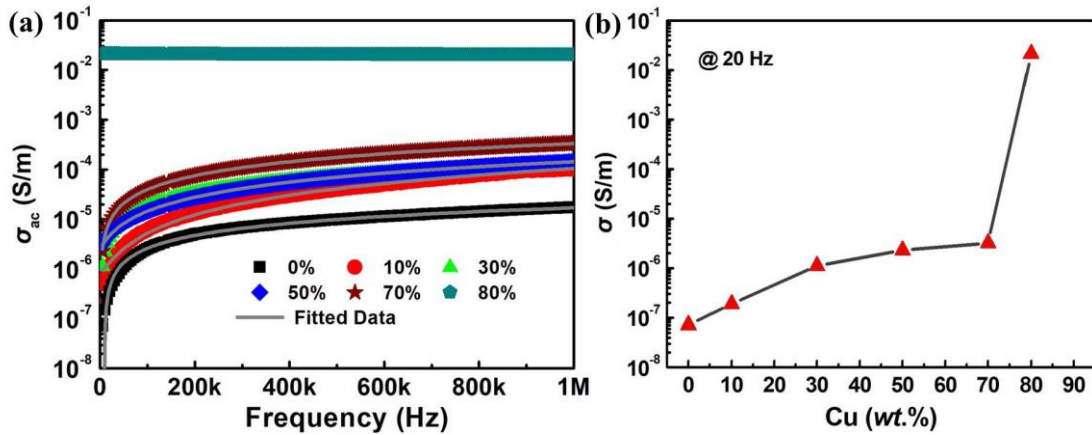


Fig. 4. The permittivity spectra of the Cu/EP composites with different Cu content (*i.e.*, 0-80 wt.%). (a) and (b) show the positive and negative permittivity spectra, respectively.

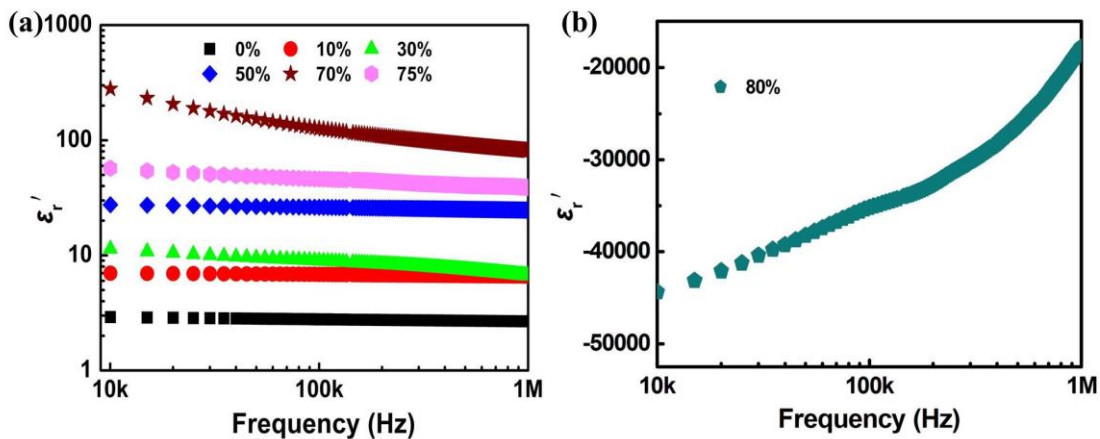


Fig. 5. The complex impedance spectra of the Cu/EP composites below (a) and above (b) the percolating state. The equivalent circuits are shown in the insets and the solid lines show the fitted

results.

